Ore Geology Reviews 149 (2022) 105091

Contents lists available at ScienceDirect

Ore Geology Reviews

journal homepage: www.elsevier.com/locate/oregeorev

# The solubility and speciation of gold in ammonia-bearing aqueous solutions at elevated temperature: An experimental study

Xin-Song Wang [a,b], A.E. Williams-Jones [b], Xian-Wu Bi [a], Zi-Qi Jiang [a], Lin-Bo Shang [a,b,*]

[a] State Key Laboratory of Ore Deposits Geochemistry, Institute of Geochemistry, Chinese Academy of Sciences, Guiyang 550081, China
[b] Department of Earth & Planetary Sciences, McGill University, 3450 University Street, Montreal, QC H3A 0E8, Canada

ARTICLE INFO

*Keywords:*
Gold solubility and speciation
Ammonium
Hydrothermal systems
Gold mineralization

ABSTRACT

The discovery, using short wavelength infrared radiation (SWIR), that some low-sulfidation epithermal gold deposits are associated with hydrothermal alteration involving ammonium minerals, particularly buddingtonite ($(NH_4)AlSi_3O_8$), has led to the suggestion that the gold may have been transported as a complex involving ammonia ($NH_3$). The speciation of gold in ammonia-rich solutions, however, has received little attention from experimentalists and, consequently, it is not known whether gold forms stable complexes with $NH_3$ and whether such species could contribute significantly to the transport of gold in epithermal ore-forming systems. To resolve this issue, we have conducted experiments to investigate the speciation and solubility of gold in ammonia-bearing solutions at temperatures of 225 and 250 °C under vapour-saturated water pressure with oxygen fugacity buffered by the assemblage magnetite-hematite. Based on the results of these experiments, gold does form stable species with ammonia at elevated temperature. The gold is interpreted to have been dissolved predominantly as $Au(NH_3)OH^0$ in solutions with a $NH_3^0$ concentration of 0.005 ~ 0.49 m and a pH(T) of 3.29 ~ 7.47. This species formed via the reaction, $Au_{(s)} + NH_{3\,(aq)} + H_2O = Au(NH_3)OH_{(aq)} + 1/2\ H_{2\,(g)}$ The logarithms of the equilibrium constant for this reaction are −8.95 ± 0.84 and −7.71 ± 0.85 for 225 and 250 °C, respectively. In order to determine whether this species is important for the transport of gold in epithermal systems, we modeled the speciation of gold in a fluid at conditions typical of those epithermal gold depositing fluids. This modeling shows that the solubility of gold as $AuHS^0$ and $Au(HS)_2^-$ is much higher than that as $Au(NH_3)OH^0$ except in alkaline ammonia-bearing fluids. The association of gold mineralization with hydrothermal alteration involving the formation of ammonium-bearing minerals in the deposits is therefore probably unrelated to the transport of gold as a Au-$NH_3$ complex but simply reflects the high concentration of $NH_4^+$ in the ore-forming fluid.

## 1. Introduction

Numerous studies have shown that low-sulfidation epithermal Au deposits form as a result of the boiling, at relatively low temperature (150–300 °C), of low salinity aqueous liquids having intermediate pH and relatively low oxygen fugactity (White and Hedenquist, 1995; Hedenquist et al., 2000; John et al., 2003; Simmons et al., 2005 and references therein). As a result of the low oxygen fugacity, sulfur is present in the liquid dominantly as $HS^-$, which forms strong complexes with gold (Shenberger and Barnes, 1989; Loucks and Mavrogenes, 1999; Williams-Jones et al., 2009; Williams-Jones and Migdisov, 2014; Hu et al., 2022). This has led to the conclusion that the gold is transported as the species $Au(HS)_2^-$ prior to boiling, and during boiling is deposited due to the loss of $H_2S$ to the vapor and the resulting destabilization of this species (Clark and Williams-Jones, 1990; Williams-Jones et al., 2009). Significantly, stable isotope (S, C, O, and H) studies indicate that the ore-forming fluids are dominated by meteoric water and that, in some cases, this water has interacted extensively with organic matter (Simmons et al., 2005; Hayashi et al., 2001; John et al., 2003; Benavente et al., 2013). This explains why some geothermal waters (considered to be analogues of the ore fluids for low sulfidation epithermal deposits) contain elevated concentrations of $NH_4^+$ (up to ~0.1 m)(Valentino et al., 1999; Holloway et al., 2011; Pirajno, 2020). It may also explain why, in some low sulfidation epithermal deposits, the ammonium feldspar, buddingtonite [$(NH_4)AlSi_3O_8$], and the ammonium mica, tobelite [$(NH_4,K)Al_2(Si_3Al)O_{10}(OH)_2$] replaces adularia and illite (or muscovite) as the dominant alteration minerals (Erd et al., 1964; Browne, 1978; Ridgway et al., 1990; Ridgway et al., 1991; Krohn et al., 1993; Hovis

* Corresponding author at: State Key Laboratory of Ore Deposits Geochemistry, Institute of Geochemistry, Chinese Academy of Sciences, Guiyang 550081, China.
*E-mail address:* shanglinbo@vip.gyig.ac.cn (L.-B. Shang).

https://doi.org/10.1016/j.oregeorev.2022.105091
Received 22 April 2022; Received in revised form 17 July 2022; Accepted 2 September 2022
Available online 6 September 2022

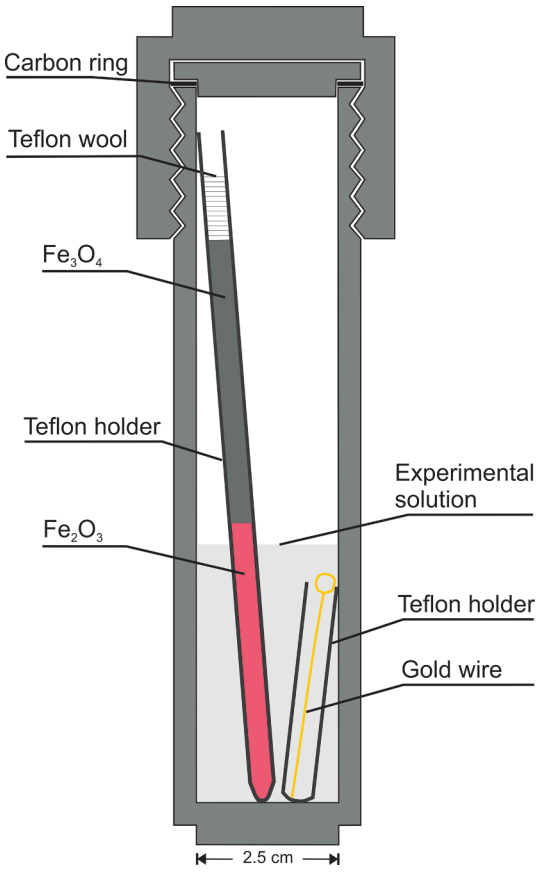


**Fig. 1.** A schematic diagram showing the experimental set-up employed in this study.

et al., 2004; Harlap, 2008; Soechting et al., 2008; Canet et al., 2015; Simpson and Christie, 2019).

The association of ammonium-bearing alteration minerals with low-sulfidation epithermal Au mineralization raises the question of whether the gold could have been transported as ammonia-bearing aqueous complexes. Indeed, such transport is predicted by the theoretical calculations of Wood et al. (1992) and was proposed by Harlap (2008) for a low sulfidation epithermal Au deposit with associated buddingtonite-tobelite alteration. The calculations of Wood et al. (1992), which involved isocoulombic extrapolations to 300 °C of potentiometric data collected at 25 °C (Skibsted and Bjerrum (1974), showed that the solubility of Au is relatively high (ppb to ppm levels) in $NH_3$-bearing aqueous fluids and reaches a maximum at the $NH_3$-$NH_4^+$–$N_2$ triple point as the species $Au(NH_3)_2^+$. Support for the notion that $Au(NH_3)_2^+$ is the dominant species in aqueous-ammonia solutions was subsequently provided in an extended X-ray adsorption fine structure (EXAFS) study by Nilsson et al. (2006), albeit for ambient temperature. However, recent studies using in situ X-ray absorption spectroscopy (XAS) at elevated temperature and ab initio molecular dynamics (MD) simulations have concluded that Au-$NH_3$ species are not important in transporting gold in ore-forming fluids because of the large competitive advantage of the bisulfide ligand in gold complexation (Liu et al., 2014; Mei et al., 2020). On the other hand, the simulations of Mei et al. (2020) show that the mixed ligand species $[Au(NH_3)(OH)]^0$ could play a role in transporting gold in sulfur-poor hydrothermal fluids.

The purpose of this paper is to report the results of an experimental study of the solubility and speciation of gold in the system $NH_4Cl$-NaCl-NaOH-$H_2O$ at temperatures up to 250 °C and near neutral to alkaline pH, and assess the potential importance of ammonia to the formation of hydrothermal gold deposits. The results of these experiments show that $Au(NH_3)OH^0$ is the dominant species at the conditions investigated, supporting the results of the ab initio calculations reported by Mei et al. (2020). Based on the thermodynamic properties for $Au(NH_3)OH^0$, retrieved from our experiments, we model the solubility of gold in an $NH_3$– and $H_2S$-bearing hydrothermal fluids and show how gold is likely transported in ammonia-rich epithermal ore-forming fluids.

## 2. Methods

### 2.1. Experiments

The experimental equipment and methods employed in this study are the same as those used in previous studies at McGill University (e.g., Migdisov and Williams-Jones, 2007; Wang et al., 2019). The experiments were carried out in batch-type titanium grade 2 autoclaves (Fig. 1) and heated in a Fisher Isotemp oven equipped with a stainless-steel box to reduce thermal gradients. Prior to each experiment, the autoclaves were cleaned by filling them with 50 wt% aqua regia ($HNO_3$: HCl, 1:3 v/v trace metal grade) for 24 h, and finally with nano-pure water. This treatment ensured that no gold from previous experiments remained on the walls of the autoclaves.

The solubility of gold wire was investigated in 0.5 m NaCl aqueous solutions of variable $NH_3$ concentration and pH at temperatures of 250 and 225 °C, and vapor-saturated water pressure. The $NH_3$-bearing solutions were prepared by adding $NH_4Cl$ solid to produce concentrations ranging from 0.005 mol/kg to 0.50 mol/kg and the pH(25 °C) of the solutions was made to vary between 5.98 and 10.98 by the addition of NaOH. The concentrations of $NH_3$ and $NH_4^+$ and the pH values of the solutions were controlled by the following reaction:

$$NH_4^+ + OH^- = NH_{3,aq} + H_2O \quad (1)$$

$$Log\ K_1 = logaNH_{3,aq} - logaNH_4^+ - logaOH^-$$

Then, the activity of ammonia in the solutions can be calculated using the equation:

$$LogaNH_{3,aq} = logaNH_4^+ + pH - log\ K_w + log\ K_1 \quad (2)$$

where log $K_w$ is the logarithms of the equilibrium constant of water.

Thus, the ratio between $NH_4^+$ and $NH_3^0$ is mainly dependent on the pH of the solutions. As the predominance boundary between $NH_4^+$ and $NH_3^0$ is ~5 at 225–250 °C (calculated using the unitherm program of the HCh software package; Shvarov, 2008), the pH of the solutions was >5 at the conditions of the experiments and the dominant nitrogen species was $NH_3^0$. All the experimental solutions and $NH_4Cl$ standards were newly prepared before each experiment. The solid reactant (gold wire; Alfa Aesar 99.999 % purity) was introduced into a small Teflon holder (~3.5 cm long). Oxygen fugacity was buffered by the assemblage magnetite-hematite, which was introduced as $Fe_3O_4$ (black powder; Alfa Aesar, 97 % purity) and $Fe_2O_3$ (Red powder; Alfa Aesar, 99 % purity) into a long Teflon holder (~11 cm; Fig. 1). At the beginning of each experiment, the two Teflon holders were placed in an autoclave and 20 ml of ammonia-bearing NaCl solution was added to them. At the conditions of the experiments, this amount was predicted to cover the holder containing the gold wire but not that containing the buffer (Fig. 1). Sets of experiments were also conducted with solutions containing variable concentrations of NaCl but no $NH_3$; the pH(25 °C) of these solutions was in the range 3 to 8 and was controlled by the addition of HCl or NaOH. These experiments were carried out using the same set-up at the same temperature and oxygen fugactiy as the experiments with $NH_3$.

The experiments were conducted for a duration of 25 days, which is significantly longer than the time required to produce a steady state concentration, based on the results of previous sets of kinetic experiments measuring metal solubility (commonly < 10 days; Shenberger and Barnes, 1989; Gibert et al., 1998; Loucks and Mavrogenes, 1999; Stefánsson and Seward, 2004). At the end of each set of experiments, the autoclaves (three in the same oven) were removed from the oven and

**Table 1**
Compositions of quenched experimental solutions from experiments. The values of pH (T), $aNH_{3,aq}$ (T), and $aNH_4^+$ (T) were calculated for the temperatures of interest.

| T (°C) | NaCl (m) | $NH_4Cl$ (m) | Au (ppb) | NaOH (m) | HCl (m) | pH (25 °C) | pH (T) | $aNH_{3,aq}$ (T) | $aNH_4^+$ (T) |
|---|---|---|---|---|---|---|---|---|---|
| 250 | 0.5 | 0.0109 | 0.79 | 0.0000646 | | 7.18 | 4.01 | 0.00032 | 0.0050 |
| 250 | 0.5 | 0.00470 | 1.11 | 0.000883 | | 8.76 | 4.90 | 0.00090 | 0.0018 |
| 250 | 0.5 | 0.0107 | 2.12 | 0.00418 | | 9.20 | 5.32 | 0.0041 | 0.0031 |
| 250 | 0.5 | 0.0812 | 5.91 | 0.0570 | | 9.77 | 5.89 | 0.056 | 0.011 |
| 250 | 0.5 | 0.0549 | 5.74 | 0.0366 | | 9.70 | 5.82 | 0.036 | 0.0086 |
| 250 | 0.5 | 0.194 | 12.9 | 0.146 | | 9.89 | 6.02 | 0.14 | 0.022 |
| 250 | 0.5 | 0.409 | 13.6 | 0.305 | | 9.88 | 6.02 | 0.29 | 0.044 |
| 250 | 0.5 | 0.499 | 14.8 | 0.376 | | 9.89 | 6.05 | 0.36 | 0.051 |
| 250 | 0.5 | 0.303 | 5.34 | 0.137 | | 9.32 | 5.46 | 0.13 | 0.072 |
| 250 | 0.5 | 0.266 | 2.63 | 0.0425 | | 8.69 | 4.83 | 0.041 | 0.10 |
| 250 | 0.5 | 0.337 | 1.0 | 0.000122 | | 5.98 | 3.29 | 0.0018 | 0.14 |
| 250 | 0.5 | 0.392 | 12.3 | 0.286 | | 9.84 | 5.98 | 0.28 | 0.045 |
| 250 | 0.5 | 0.401 | 11.0 | 0.295 | | 9.85 | 6.00 | 0.28 | 0.045 |
| 250 | 0.525 | | 0.66 | | | 5.68 | | | |
| 250 | 0.55 | | 0.59 | | | 5.68 | | | |
| 250 | 0.575 | | 0.49 | | | 5.67 | | | |
| 250 | 0.7 | | 0.69 | | | 5.65 | | | |
| 250 | 0.8 | | 0.63 | | | 5.63 | | | |
| 250 | 0.8 | | 0.64 | | | 5.63 | | | |
| 250 | 0.5 | | 0.12 | | 0.000514 | 3.48 | 3.71 | | |
| 250 | 0.5 | | 0.34 | | 0.000922 | 3.22 | 3.46 | | |
| 250 | 0.5 | | 0.32 | | 0.000525 | 3.47 | 3.70 | | |
| 250 | 0.5 | | 0.52 | | 0.0000029 | 5.73 | 5.51 | | |
| 225 | 0.5 | 0.488 | 1.15 | 0.391 | | 10.01 | 6.41 | 0.37 | 0.045 |
| 225 | 0.5 | 0.422 | 3.06 | 0.352 | | 10.11 | 6.51 | 0.34 | 0.032 |
| 225 | 0.5 | 0.348 | 1.87 | 0.288 | | 10.09 | 6.48 | 0.28 | 0.028 |
| 225 | 0.5 | 0.218 | 2.48 | 0.214 | | 10.98 | 7.47 | 0.21 | 0.0022 |
| 225 | 0.5 | 0.285 | 0.77 | 0.168 | | 9.56 | 5.95 | 0.16 | 0.056 |
| 225 | 0.5 | 0.409 | 1.05 | 0.339 | | 10.09 | 6.48 | 0.32 | 0.033 |
| 225 | 0.5 | 0.397 | 1.55 | 0.326 | | 10.07 | 6.46 | 0.31 | 0.033 |
| 225 | 0.5 | 0.060 | 0.35 | 0.047 | | 9.96 | 6.33 | 0.046 | 0.0066 |
| 225 | 0.5 | 0.0415 | 0.37 | 0.0327 | | 9.96 | 6.34 | 0.032 | 0.0045 |
| 225 | 0.5 | 0.0103 | 0.23 | 0.0050 | | 9.38 | 5.76 | 0.0049 | 0.0027 |
| 225 | 0.5 | | 0.08 | | 0.000273 | 3.75 | 3.92 | | |
| 225 | 0.6 | | 0.09 | | 0.000350 | 3.65 | 3.83 | | |
| 225 | 0.7 | | 0.23 | | 0.0000610 | 4.42 | 4.60 | | |
| 225 | 0.8 | | 0.31 | | 0.00000498 | 5.51 | 5.43 | | |
| 225 | 0.9 | | 0.23 | | 0.00000480 | 5.43 | 5.41 | | |
| 225 | 0.5 | | 0.03 | | 0.0000105 | 5.17 | 5.24 | | |
| 225 | 0.5 | | 0.02 | | 0.00000400 | 5.59 | 5.45 | | |
| 225 | 0.5 | | 0.03 | 0.00000062 | | 7.60 | 5.62 | | |
| 225 | 0.5 | | 0.04 | | 0.00000530 | 5.46 | 5.40 | | |
| 225 | 0.5 | | 0.13 | | 0.000143 | 4.03 | 4.20 | | |
| 225 | 0.5 | | 0.37 | | 0.0000204 | 4.88 | 5.02 | | |

quenched to ambient temperature in less than 15 min. The long Teflon holders containing the oxygen buffer and the gold wire were then removed from the autoclaves; the small holders were left in the autoclaves. A 1 ml aliquot of solution was taken from each autoclave for the determination of pH, which was carried out in less than 5 min. This was followed by the removal of a 1 ml aliquot of solution, which was introduced into a test tube containing 0.1 ml HCl (~36.5 wt%, trace metal grade) for analysis of the ammonia concentration, which was carried out less than 2 h after the completion of the experiments; the acidification was necessary to ensure that all the $NH_3$ was converted to $NH_4^+$; $NH_3$ is highly volatile, particularly at high pH. Next, 6 ml of concentrated trace metal grade aqua regia was to the autoclaves to dissolve any gold that had precipitated on the walls during quenching. After 30 min, the mixed solution was removed from the autoclaves for analysis of their gold content. The pH and ammonia concentration were measured using an accuTupH™ Rugged Bulb Combination pH Electrode and Thermo Scientific™ Orion™ High-Performance Ammonia Electrode, respectively. Prior to the ammonia analyses, 0.3 ml of blue Ionic Strength Adjuster (ISA, ThermoFisher), which provides a constant background ionic strength and adjusts the solution pH to an alkaline value, was added to each experimental and standard solution to ensure that all the dissolved $NH_3$ and $NH_4^+$ was converted to $NH_3$ gas for analysis. Ammonia standards with $NH_3$ concentrations of 0.001, 0.01, 0.1, and 0.5 mol/kg were prepared from a $NH_4Cl$ stock solution. The pH standards have pH values ranging from 5 to 13 and were prepared from a 0.5 m NaCl solution by adding to it appropriate amounts of NaOH or HCl solution. The concentration of NaOH or HCl in these standards was measured by titration. The resulting pH values were corrected to the corresponding pH values for the temperatures of the experiments using the HCh software package (Shvarov, 2008). Gold concentrations were analyzed using Inductively Coupled Plasma Mass Spectrometry after 25 times dilution of the experimental solution using a 2 wt% HCl solution. X-ray diffraction analysis confirmed that the buffer solids were both present after the experiments.

### 2.2. Data optimization

The dissolved gold species were identified from the slope of the logarithm of the molality of gold with respect to those of the ligands in the various experiments. Thermodynamic properties for these species and the standard Gibbs free energy of formation, $\Delta G^\circ_f$, were determined from the molality of Au, $NH_4Cl$, NaCl and NaOH in each experiment using the program OptimA (masses corresponding to the excess amounts of solute, gold, and the oxygen buffer assemblage at the end of each experiment were also specified in the input file), which is part of the HCh software package (Shvarov, 2015). The activity coefficient of each ionic species was calculated using the extended Debye-Hückel equation (Helgeson et al., 1981; Oelkers and Helgeson, 1990; Oelkers and

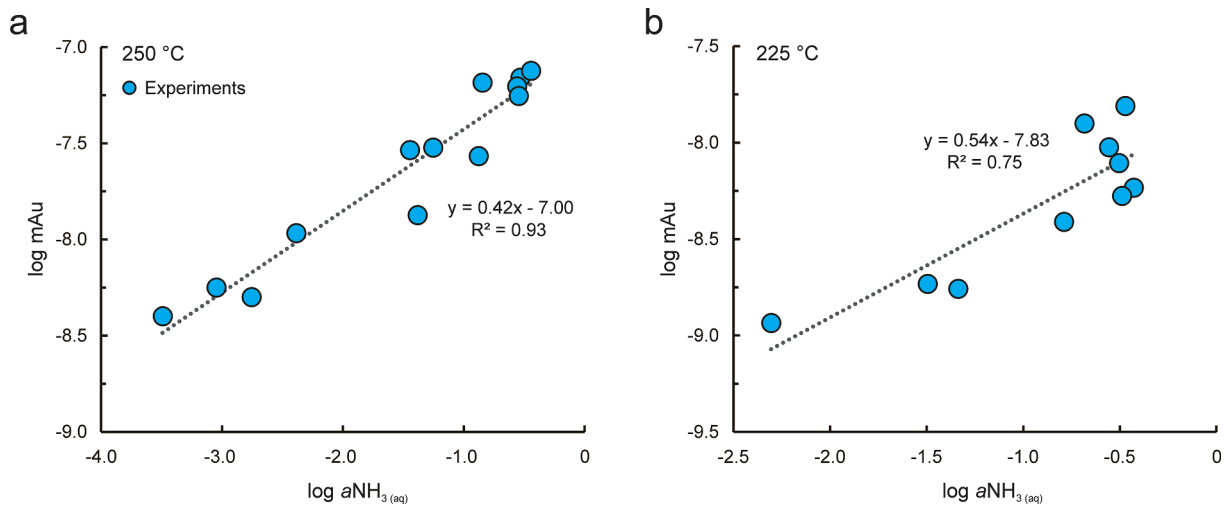


**Fig. 2.** Results of experiments with $NH_3$-bearing solutions at 250 and 225 °C showing the concentrations of dissolved gold (log mAu) as a function of the activity of $NH_3$ (log $aNH_3$). The equations "y = ax - b" represent linear regressions of the data.

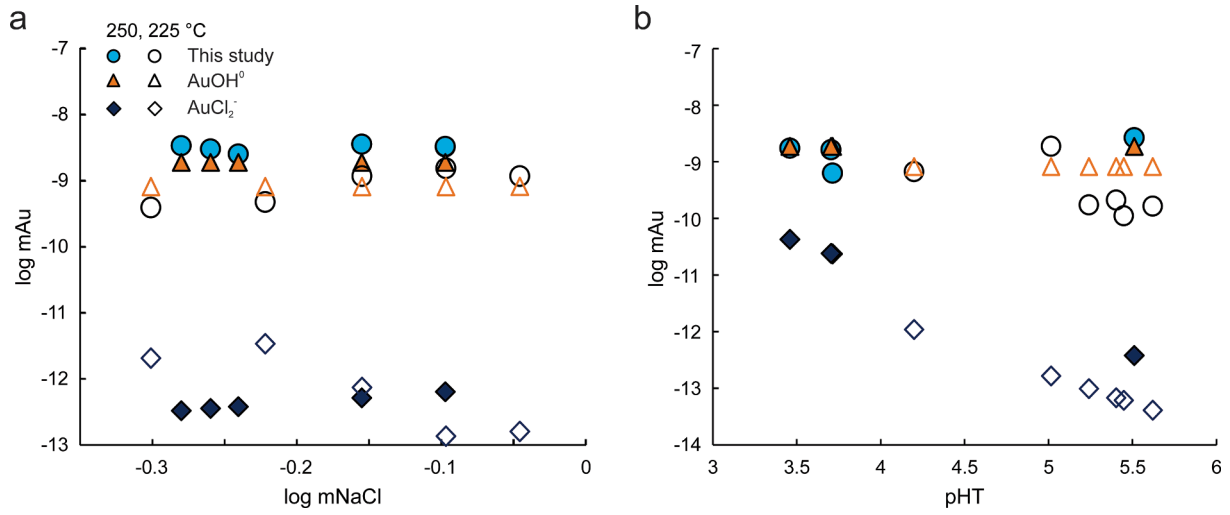


**Fig. 3.** Diagrams showing the log molality of Au versus a) log mNaCl and b) pHT at 250 (filled symbol) and 225 (open symbol) °C for NaCl-$H_2O$ fluids with no $NH_3$. The solubility of the gold as the species $Au(OH)^0$ and $AuCl_2^-$ was calculated using the thermodynamic data of Akinfiev and Zotov (2001).

Helgeson, 1991):

$$log\gamma_n = -\frac{A \bullet [z_n]^2 \bullet \sqrt{I}}{1 + B \bullet \mathring{a} \bullet \sqrt{I}} + b_\gamma \bullet I + \Gamma \quad (3)$$

in which A and B are constants representing Debye-Hückel limiting law parameters, $b_\gamma$ is the extended parameter for NaCl from Helgeson and Kirkham (1974), $\mathring{a}$ is the distance of closest approach, which is specific to the ion of interest, $z$ is the charge of the ion, $\Gamma$ is a molarity to molality conversion factor, and $I$ is the ionic strength calculated using Equation (4):

$$I = \frac{1}{2}\sum_{i=1}^{n} c_i z_i^2 \quad (4)$$

where $c_i$ is the molar concentration of ion i (mol/kg) and $z_i$ is the charge of that ion. Parameter $I$ represents the true ionic strength as all the dissolved components were considered. The activity coefficients of neutral species were assumed to be unity. The Haar-Gallagher-Kell and Marshall and Franck models were used to determine the thermodynamic properties and dissociation constant of $H_2O$, respectively, for the experimental conditions (Marshall and Franck, 1981; Kestin et al., 1984).

## 3. Results

### 3.1. Identification of the dissolved gold species

The results of the experiments at 250 and 225 °C are reported in Table 1. In order to determine whether or not gold solubility depends on ammonia concentration, sets of experiments were conducted with solutions having variable ammonia concentration. From Fig. 2, it is evident that the concentration of gold increases linearly with log $aNH_3^0$; the slopes are 0.54 and 0.42 for 225 and 250 °C, respectively. As the solutions used to evaluate the effect of $NH_3$ on gold solubility also contained NaCl, and pH was varied using NaOH, separate sets of experiments were conducted in which the solutions had variable concentrations of NaCl and variable pH but no $NH_3$. The results for a set of these experiments at a constant pH (T) of ~5.6 show that the solubility of gold is independent of the chloride concentration and one to two orders of magnitude higher than the calculated solubility of the species $AuCl_2^-$ (Akinfiev and Zotov, 2001), indicating that Au-Cl species did not contribute to the solubility of gold in the $NH_3$-bearing solutions (Fig. 3).

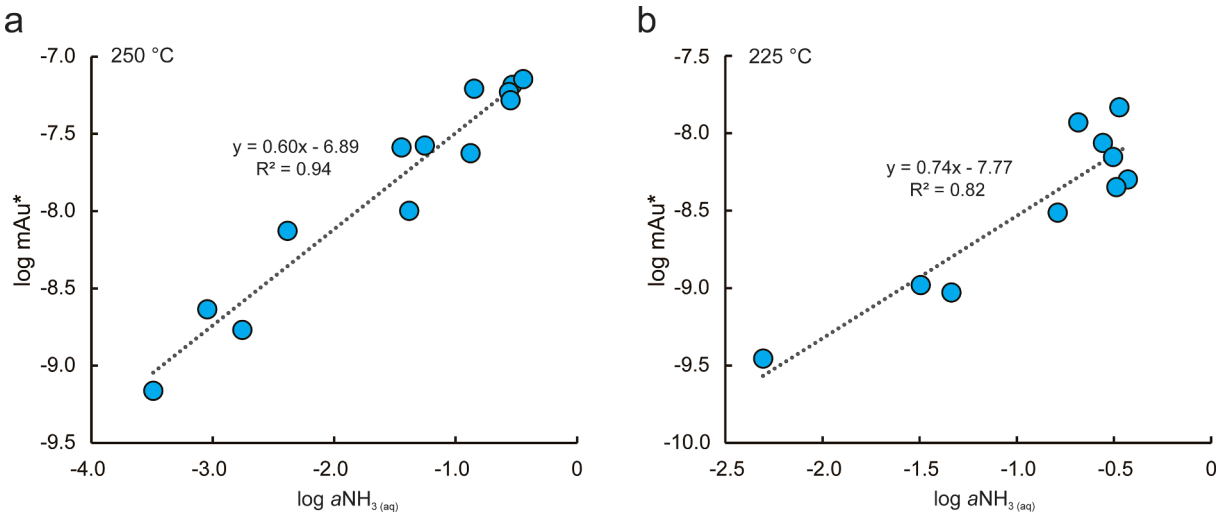


**Fig. 4.** Diagrams showing the log molality of Au (Au*) versus log $aNH_3$ at 250 and 225 °C after subtraction of the contribution of $Au(OH)^0$ to the total gold concentration. This contribution was calculated using the average value for the concentration of Au in the 0.5 m NaCl solutions containing no $NH_3$. The dotted lines represent linear regressions to the data and "y = ax - b" the equations of these lines.

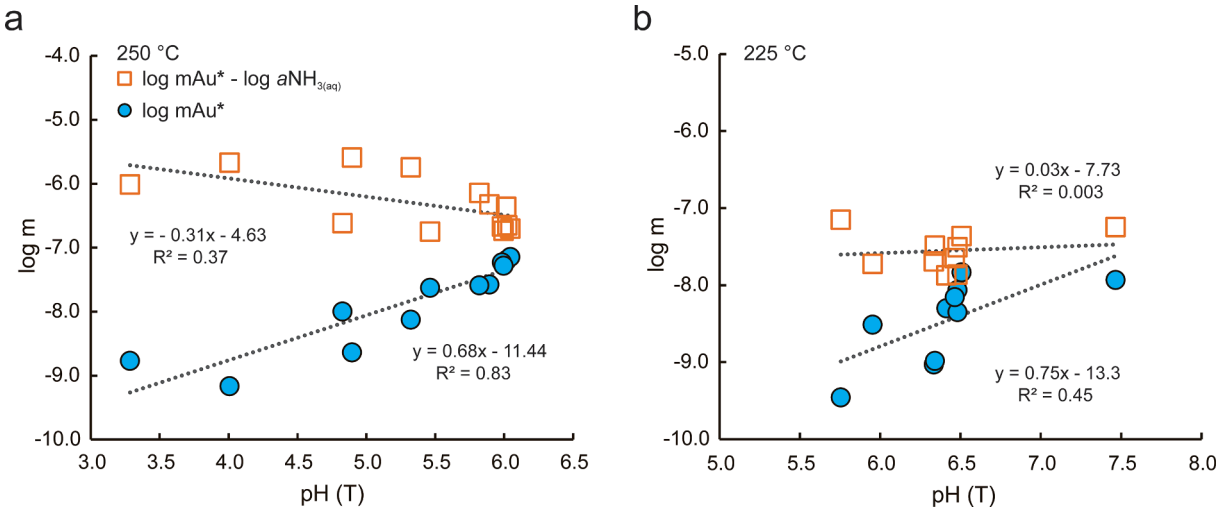


**Fig. 5.** Plots of (log mAu* – log $aNH_3$) and log mAu versus pH (T) at 250 and 225 °C. The filled blue circles represent the results of the experiments and the open red squares represent the values of (log mAu* – log $aNH_3$). The term Au* refers to the total concentration of Au obtained in the experiments minus its concentration as the species $AuOH^0$. The latter was calculated with thermodynamic data from Akinfiev and Zotov (2001). The dotted lines represent the linear regressions to the data for (log mAu – log $aNH_3$) and log mAu versus pH at the different temperatures and "y = ax-b" the equations of these lines. (For interpretation of the references to colour in this figure legend, the reader is referred to the web version of this article.)

In contrast, the experimental solubility of gold is almost equal to the calculated solubility of $AuOH^0$ using the thermodynamic data from Akinfiev and Zotov (2001) (Fig. 3a). Therefore, $AuOH^0$ is most likely the dominant species in the NaCl solutions without $NH_3$. We subtracted the concentration of the species $AuOH^0$ from the gold concentration of each experimental data point and show the resulting gold concentration (log mAu*) versus log $aNH_3^0$ in Fig. 4. The result is an increase in the slopes from those shown in Fig. 2 to 0.74 and 0.60 for 225 and 250 °C, respectively (Fig. 4), suggesting a species with a ligand number of unity, i.e., having one $NH_3$ molecule for each gold atom. It is noteworthy, however, that although the log mAu* values also increase with pH(T) (Fig. 5), they are independent of pH(T) once the Au* concentrations are corrected for the effect of $NH_3$ (deducting the contribution of ammonia with respect to the formation of a species with ammonia and gold atoms in a ratio of 1:1) (Fig. 5).

Considering that the species reponsible for the solubility of gold in our experiments is inferred to contain one $NH_3$ molecule per gold atom, this species could be $Au(NH_3)^+$, as inferred from theoretical extrapolations from ambient temperature (Wood et al., 1992) and ab initio calculations (Mei et al., 2020). The problem with this interpretation, however, is the lack of a correlation with pH. An alternative is the mixed species, $Au(NH_3)(OH)^o$, proposed by Mei et al. (2020). This species is interpreted to have formed via the pH-independent redox reaction:

$$Au_{(s)} + NH_{3\ (aq)} + H_2O = Au(NH_3)(OH)_{(aq)} + 1/2\ H_{2\ (g)} \quad (5)$$

$$Log\ K_3 = logaAu(NH_3)(OH)^0 - logaNH_3^0 + 1/2\ logfH_2$$

In the absence of evidence to the contrary, we have assumed that our data reflect dominance of the solubility of gold in our experiments by the species $Au(NH_3)(OH)^0$ and we have used them to calculate stability constants for this species, which we compare to those reported by Mei et al. (2020).

**Table 2**
Gibbs free energies of formation ($\Delta G_f^\circ$) and stability constants (Log β) for the gold species identified in this study and a previous study.

| $Au(NH_3)OH^0$ | 250 °C | 225 °C | References |
|---|---|---|---|
| $\Delta G_f^\circ$ | −234.35 ± 23.44 | −219.89 ± 21.99 | This study |
| | −215.73 | −208.54 | Mei et al., 2020 |
| Log β | 17.82 ± 1.78 | 17.54 ± 1.75 | This study |
| | 15.96 | 16.34 | Mei et al., 2020 |

**Table 3**
Logarithms of equilibrium constants (Log K) and their associated uncertainty for the Au dissolution reaction investigated in this study.

| LogK | 250 °C | 225 °C |
|---|---|---|
| $Au_{(s)} + NH_{3\,(aq)} + H_2O = Au(NH_3)OH_{(aq)} + 1/2\,H_{2\,(g)}$ | −7.71 ± 0.85 | −8.95 ± 0.84 |

### 3.2. Evaluation of the Gibbs free energy of formation ($\Delta G_f^\circ$)

The standard Gibbs free energy for $Au(NH_3)(OH)^0$ was determined from the molality of gold, $NH_4Cl$, NaCl, and NaOH in each experiment using the program OptimA in the HCh software package (Shvarov, 2015); the molality of NaOH was calculated from the starting NaCl concentration and the pH and $NH_3$ concentration measured after each experiment. In addition to the species, $Au(NH_3)(OH)^0$, the following aqueous species were also considered in the calculations: $O_2$, $H_2$, $H^+$, $OH^-$, $Na^+$, $Cl^-$, $NH_3^0$, $NH_4^+$, $NaOH^0$, $NaCl^0$, $HCl^0$, $Au^+$, $AuOH^0$, $Au(OH)_2^-$, $AuCl^0$, $AuCl_2^-$, $AuCl_3^{2-}$, $AuNH_3^+$, and $Au(NH_3)_2^+$. Thermodynamic data for these species were obtained from Johnson et al. (1992), Shock et al. (1997), Sverjensky et al. (1997), Akinfiev and Zotov (2001), Akinfiev and Zotov (2010), and Mei et al. (2020), and values for the extended parameter for NaCl were taken from Oelkers and Helgeson (1991). Thermodynamic data for the gold and iron oxide solids (hematite and magnetite) were taken from Robie and Hemingway (1995). Hydrogen fugacity was calculated from Reaction (6).

$$2Fe_3O_{4\ (s)} + H_2O_{(g)} = 3Fe_2O_{3\ (s)} + H_{2\ (g)} \quad (6)$$

$$Log\ K_4 = logfH_2 - logfH_2O$$

The Gibbs free energy for the formation of $Au(NH_3)(OH)^0$:

$$Au^+ + NH_3^0 + OH^- = Au(NH_3)OH^0 \quad (7)$$

was calculated using the standard Gibbs free energy of $Au(NH_3)(OH)^0$ (see above) and the standard Gibbs free energy of the other species involved in the reaction, namely $Au^+$, $NH_3^0$, and $OH^-$ (Akinfiev and Zotov, 2001; and Shock et al. 1997). The sources of these data are listed in Appendix 1. The formation constant (log β) was calculated using the relationship $\Delta G^\circ$ = -RTlnK; the standard Gibbs free energy, the formation constant, and the uncertainty associated with their determination, were calculated using the OptimA program and are reported in Table 2. Using this formation constant, we calculated the equilibrium constant (log K) for the gold dissolution reaction reported in Table 3. Uncertainties in the equilibrium constants were determined by calculating the log K values for each data point using Reactions (5) and (7), and then calculating the standard deviation of these values, for each temperature.

## 4. Discussion

### 4.1. Comparison to previous studies

As discussed earlier, several studies have evaluated the solubility of gold in ammonia-bearing aqueous solutions. Based on extrapolations to 300 °C of potentiometric data collected at 25 °C, Wood et al. (1992) concluded that $Au(NH_3)_2^+$ is the dominant ammonia-bearing gold species in ore-forming hydrothermal fluids, a conclusion that was reinforced by the EXAFS study of Nilsson et al. (2006). The results of our experiments confirm that gold solubility increases strongly with ammonia activity. However, they provide no evidence for a Au-$NH_3$ species with a ligand number of 2 and, instead, indicate that the ligand number of ammonia in the dominant aqueous gold species is 1. Moreover, they suggest that this species is a mixed hydroxide ammonia species with the stoichimometry $Au(NH_3)(OH)^0$. The same conclusion was reached by Mei et al. (2020), based on the results of ab initio simulations. The formation constants extracted from our data for this species are 17.54 and 17.82 at 225 °C and 250 °C, respectively (Table 2). By comparison, the simulations of Mei et al. (2020) yielded formation constants (log β values) for the species of 16.3 and 16.0, which, although somewhat lower than the values obtained from our experiments, are indistinguishable from them within the uncertainty of the determinations (Fig. 6).

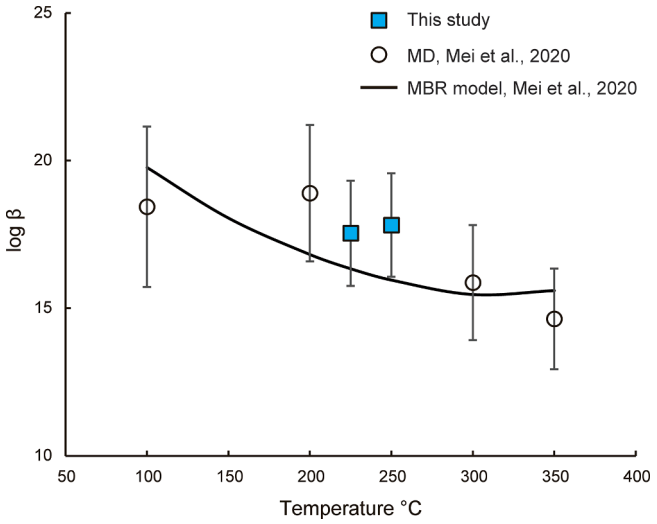


**Fig. 6.** A plot of log β versus temperature. The filled blue squares represent the results of this study, the open circles are the results of *ab initio* molecular dynamics simulations (MD) from Mei et al. (2020) and the black line represents the calculated log β values based on the parameters for the MBR model presented by Mei et al. (2020). (For interpretation of the references to colour in this figure legend, the reader is referred to the web version of this article.)

### 4.2. Application to natural systems

As discussed in the introduction to this paper, some low-sulphidation epithermal Au deposits are associated with the ammonium minerals, buddingtonite and tobelite rather than adularia and illite/muscovite, respectively (Canet et al., 2015; Harlap, 2008; Krohn et al., 1993; Ridgway et al., 1990; Ridgway et al., 1991; Simpson and Christie, 2019; Soechting et al., 2008). The fluids forming low sulfidation deposits have low salinity <5 wt% NaCl, and relatively high $H_2S$ contents (10 s to 100 s ppm) at near-neutral and neutral pH and a temperature of 150–300 °C (Simmons et al., 2005 and references therein). The results of stable isotope studies (S, C, O, and H) suggest that the fluids mainly comprise deeply circulated meteoric water that has interacted with organic matter, which typically has high contents of nitrogen-rich compounds (Hayashi et al., 2001; John et al., 2003; Benavente et al., 2013). By analogy with some geothermal fluids, these fluids may contain elevated concentrations of $NH_3$ (up to 0.1 m; Valentino et al., 1999; Holloway et al., 2011; Pirajno, 2020). It is thus attractive to propose that, in some cases, the species $Au(NH_3)(OH)^0$ may play an important role in the transport of gold in ore-forming low sulfidation epithermal systems. Here, we make use of the thermodynamic data presented earlier and data for other gold species to model gold transport in ammonia-rich hydrothermal fluids at 250 °C.

In order to simulate an ammonia-rich epitherml system, we assumed

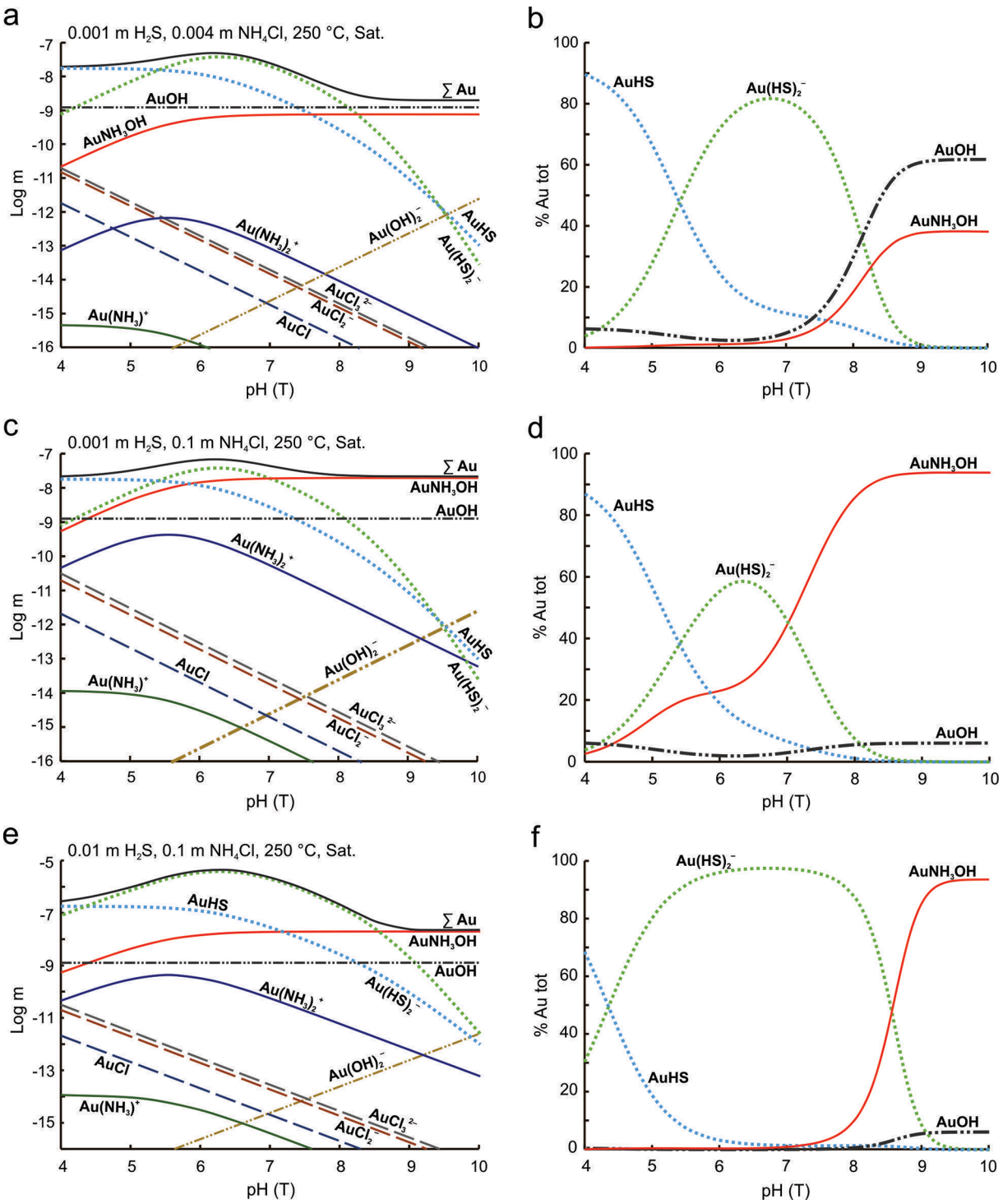


**Fig. 7.** (a), (c), and (e) Plots showing the concentration of aqueous species and gold solubility as a function of increasing pH (T). The fluid in (a), (c), and (e) contained 0.5 m NaCl and 0.25 m HCl, at 250 °C, and vapor-saturated water pressure. The initial pH of the fluid was 4. It was saturated with respect to gold. Fluid (a) contained 0.001 m $H_2S$ and 0.004 m $NH_4Cl$, (c) 0.001 m $H_2S$ and 0.1 m $NH_4Cl$, and (e) 0.1 m $H_2S$ amd 0.1 m $NH_4Cl$, respectively. The fluid was titrated with NaOH to produce the pH increase. (b), (d), and (f) display the proportions of AuHS, $Au(HS)_2^-$, AuOH, and $AuNH_3OH$ in the fluids corresponding to (a), (c), and (e), respectively, as a function of pH. The sum of the concentration of the four gold species in (b), (d), and (f) represents up to ~95 % of the total gold concentration. Thermodynamic data for the gold species were taken from this study, Sverjensky et al. (1997), Akinfiev and Zotov (2001), Akinfiev and Zotov (2010), and Mei et al., (2020).

that the ore-forming liquid is at the pressure of vapour saturation, that it contains 0.5 m NaCl, that the pH was initially 4 and that the oxygen fugacity was buffered by the mineral assemblage, magnetite-pyrite-pyrrhotite ($fO_2$ = -36.49 at 250 °C). The modeling was carried out for three series of solution, containing (1) 0.001 m $H_2S$ and 0.004 m $NH_4Cl$, (2) 0.001 m $H_2S$ and 0.1 m $NH_4Cl$, and (3) 0.01 m $H_2S$ and 0.1 m $NH_4Cl$, to compare the relative contributione of the gold-ligand species Au-Cl, Au-HS, Au-OH, and Au-$NH_3$ at variable $H_2S$ and $NH_4Cl$ concentration. As the stability of these gold species varies depending on the pH of the solutions, the pH of these solutions in each model was caused to increase by titrating with NaOH. The sources of thermodynamic data for the aqueous species used in the models are listed in Appendix 1.

In the first solution series (Fig. 7a and b), the gold dissolved as the species of $AuHS^0$ and $Au(HS)_2^-$ at a level of 100 s of ppb for pH values from 4 to 8, and its concentration decreased to a few ppb at higher pH owing to the decomposition of $AuHS^0$ and $Au(HS)_2^-$ and its dependence on the less stable species $AuOH^0$ and $Au(NH_3)OH^0$. As the concentration of $NH_3$ was low (0.004 m), the dominant species in the solution at pH values from 8 to 10 was $AuOH^0$ rather than $Au(NH_3)OH^0$. In the second series, although the molality of $NH_4Cl$ was higher (0.1 m), the results were similar to those of the first series. Thus, the gold concentration was on the order of 100 s of ppb at a pH between a pH of 4 and 7, dominantly as bisulfide species, and decreased to 10 s of ppb at a pH > 7 because of the breakdown of the gold bisulfide species (Fig. 7c and 7d). Finally, in the third series, for which the solution had the highest contents of $H_2S$ (0.01 m) and $NH_4Cl$ (0.1 m), the concentration of gold was an order of magnitude higher (several ppm) than in series 1 and 2 for pH values of 4 to 8.5 due to the greater stability of $Au(HS)_2^-$. At higher pH, the concentration decreased to 10 s of ppb due to the instability of $Au(HS)_2^-$ (Fig. 7e and f).

In summary, the above models suggest that the Au-HS species are more stable than Au-$NH_3$ and Au-OH species, and are the dominant gold complexes in these sulfur- and ammonium-bearing fluids (0.001 ~ 0.01 m $H_2S$ and 0.004 ~ 0.1 m $NH_3$) at a pH of 4 ~ 7 and 250 °C. The species of $Au(HS)_2^-$ is most important at near-neutral and slightly alkaline pH because of the high activity of $HS^-$ relative to $H_2S^0$, wheras, the gold ammonia species $Au(NH_3)OH^0$ is important only in solutions with high concentrations of $NH_3$ (>0.004 m) and a pH > 7. Thus, the results of our modelling indicate that gold is transported dominantly as bisulfide species in fluids at the mildly acidic to mildly alkaline conditions (pH < 7) thought to prevail during the formation of low-sulphidation epithermal Au deposits.

Inasmuch as boiling is considered to be the principal reason for the formation of low sulphidation epithermal deposits, because of the resulting loss of $H_2S$ to the vapor (Clark and Williams-Jones, 1990; John et al., 2003; Simmons et al., 2005; Williams-Jones et al., 2009), we propose that loss of $NH_3$ to the vapor could also be the cause of alteration of the host rocks by ammonium minerals. Specifically, we propose that reaction of $NH_3$ with hydrogen ions in the condensed acidic vapor would produce $NH_4^+$ that, on mixing of the condensate with the residual liquid, could alter the wall-rocks to buddingtonite and tobelite as analogues of the adularia and sericite that characterize other low sulphidation epithermal deposits (Erd et al., 1964; Browne, 1978; Krohn et al., 1993; Hovis et al., 2004). Although our study shows that ammonia complexes are not important in the transport of gold in low sulphidation epithermal systems, it highlights the role that ammonia potentially plays in altering the host rocks to ammonium minerals, which are easily detected by portable SWIR analyzers, and can be important pathfinders for low-sulphidation epithermal gold mineralization.

## 5. Conclusions

The results of this study show that gold dissolves as $Au(NH_3)OH^0$ in ammonia-bearing fluids at near-neutral to alkaline pH. However, gold is more stable as bisulfide species in fluids at these same conditions, which are also thought to be those that prevail during the formation of low-sulfidation epithermal Au deposits. The association of gold mineralization with hydrothermal alteration involving the formation of ammonium-bearing minerals in the deposits is therefore probably not related to the transport of gold as an Au-$NH_3$ complex but simply reflects the high concentration of ammonia in the ore-forming fluid and its conversion to $NH_4^+$ during wall-rock alteration. The main significance of buddingtonite/tobelite alteration is that it is easily detected with SWIR analyzers and is thus a potentially important pathfinder for low sulfidation epithermal gold mineralization.

**Table A1**
Sources of data used in the thermodynamic calculations.

| Species and solid phases | Formation | References |
|---|---|---|
| Aqueous species | $Au(NH_3)OH^0$ | This study |
| | $Na^+$ | Johnson et al. (1992) |
| | $H^+$ | Shock et al. (1997) |
| | $OH^-$ | Shock et al. (1997) |
| | $O_2$ | Johnson et al. (1992) |
| | $H_2$ | Johnson et al. (1992) |
| | $Cl^-$ | Johnson et al. (1992) |
| | $NaCl^0$ | Sverjensky et al. (1997) |
| | $NaOH^0$ | Shock et al. (1997) |
| | $HCl^0$ | Tagirov et al. (1997) |
| | $Au^+$ | Akinfiev and Zotov. (2001) |
| | $AuCl^0$ | Akinfiev and Zotov. (2001) |
| | $AuCl_2^-$ | Akinfiev and Zotov. (2001) |
| | $AuCl_3^{2-}$ | Sverjensky et al. (1997) |
| | $AuOH^0$ | Akinfiev and Zotov. (2001) |
| | $Au(OH)_2^-$ | Akinfiev and Zotov. (2001) |
| | $AuNH_3^+$ | Mei et al. (2020) |
| | $Au(NH_3)_2^+$ | Mei et al. (2020) |
| | $AuHS^0$ | Akinfiev and Zotov. (2010) |
| | $Au(HS)_2^-$ | Akinfiev and Zotov. (2010) |
| Gold | Au | Robie and Hemingway (1995) |
| Magnetite | $Fe_3O_4$ | Holland and Powell (2011) |
| Hematite | $Fe_2O_3$ | Holland and Powell (2011) |

## Declaration of Competing Interest

The authors declare that they have no known competing financial interests or personal relationships that could have appeared to influence the work reported in this paper.

## Data availability

Data will be made available on request.

## Acknowledgements

The experimental work described in this paper was carried out in the Fluid-Rock Interaction Laboratory, Department of Earth and Planetary Sciences, McGill University and was funded by the National Natural Science Foundation of China (91955209; 41973059); Youth Innovation Promotion Association CAS (2021398); grants from the Innovation and Entrepreneurship Project of High-level Talents Guizhou Province to XSW (2021-10); a NSERC Discovery grant to AEW-J; and an Open Research Fund of State Key Laboratory of Ore Deposit Geochemistry to AEW-J. We thank Longbo Yang, Anna Katharina Jung, and Andre Poirier for their assistance in conducting the ICP-MS analyses. The constructive reviews of Yanlu Xing and an anonymous referee helped improve the manuscript.

## Appendix

Table A1.

## References

Akinfiev, N.N., Zotov, A.V., 2001. Thermodynamic description of chloride, hydrosulfide, and hydroxo complexes of Ag (I), Cu (I), and Au (I) at temperatures of 25–500 °C and pressures of 1–2000 bar. Geochem. Int. 39 (10), 990–1006.

Akinfiev, N.N., Zotov, A.V., 2010. Thermodynamic description of aqueous species in the system Cu-Ag-Au-S-O-H at temperatures of 0–600 °C and pressures of 1–3000 bar. Geochem. Int. 48 (7), 714–720.

Benavente, O., Tassi, F., Gutierrez, F., Vaselli, O., Aguilera, F., Reich, M., 2013. Origin of fumarolic fluids from Tupungatito Volcano (Central Chile): interplay between magmatic, hydrothermal, and shallow meteoric sources. Bull. Volcanol. 75.

Browne, P., 1978. Hydrothermal alteration in active geothermal fields. Annu. Rev. Earth Planet. Sci. 6, 229–248.

Canet, C., Hernandez-Cruz, B., Jimenez-Franco, A., Pi, T., Pelaez, B., Villanueva-Estrada, R.E., Alfonso, P., Gonzalez-Partida, E., Salinas, S., 2015. Combining ammonium mapping and short-wave infrared (SWIR) reflectance spectroscopy to

constrain a model of hydrothermal alteration for the Acoculco geothermal zone, Eastern Mexico. Geothermics 53, 154–165.
Clark, J.R., Williams-Jones, A.E., 1990. Analogues of epithermal gold–silver deposition in geothermal well scales. Nature 346, 644–645.
Erd, R.C., White, D.E., Fahey, J.J., Lee, D.E., 1964. Buddingtonite, an ammonium feldspar with zeolitic water1. Am. Miner. 49, 831–850.
Gibert, F., Pascal, M.L., Pichavant, M., 1998. Gold solubility and speciation in hydrothermal solutions: experimental study of the stability of hydrosulphide complex of gold (AuHS°) at 350 to 450°C and 500 bars. Geochim. Cosmochim. Acta 62 (17), 2931–2947.
Harlap, A., 2008. Alteration and ammonium enrichment vectors to low-sulphidation epithermal mineralization: insights from the Banderas gold-silver prospect.
Hayashi, K.-I., Maruyama, T., Satoh, H., 2001. Precipitation of gold in a low-sulfidation epithermal gold deposit: insights from a submillimeter-scale oxygen isotope analysis of vein quartz. Econ. Geol. 96, 211–216.
Hedenquist, J.W., Arribas, R.A., Gonzalez-Urien, E., 2000. Exploration for epithermal gold deposits. Rev. Econ. Geol., Soc. Econ. Geologists 13, 245–277.
Helgeson, H.C., Kirkham, D.H., 1974. Theoretical prediction of the thermodynamic behavior of aqueous electrolytes at high pressures and temperatures; I, Summary of the thermodynamic/electrostatic properties of the solvent. Am. J. Sci. 274 (10), 1089–1198.
Helgeson, H.C., Kirkham, D.H., Flowers, G.C., 1981. Theoretical prediction of the thermodynamic behavior of aqueous electrolytes by high pressures and temperatures; IV, Calculation of activity coefficients, osmotic coefficients, and apparent molal and standard and relative partial molal properties to 600 degrees C and 5kb. Am. J. Sci. 281 (10), 1249–1516.
Holland, T.J.B., Powell, R., 2011. An improved and extended internally consistent thermodynamic dataset for phases of petrological interest, involving a new equation of state for solids. J. Metamorph. Geol. 29 (3), 333–383.
Holloway, J.M., Nordstrom, D.K., Böhlke, J.K., McCleskey, R.B., Ball, J.W., 2011. Ammonium in thermal waters of Yellowstone National Park: processes affecting speciation and isotope fractionation. Geochim. Cosmochim. Acta 75, 4611–4636.
Hovis, G.L., Harlov, D., Gottschalk, M., 2004. Solution calorimetric determination of the enthalpies of formation of NH4-bearing minerals buddingtonite and tobelite. Am. Miner. 89, 85–93.
Hu, M., Chou, I.M., Wang, R., Shang, L., Chen, C., 2022. High solubility of gold in H2S–H2O ± NaCl fluids at 100–200 MPa and 600–800 °C: A synthetic fluid inclusion study. Geochim. Cosmochim. Acta.
John, D.A., Hofstra, A.H., Fleck, R.J., Brummer, J.E., Saderholm, E.C., 2003. Geologic setting and genesis of the Mule Canyon low-sulfidation epithermal gold-silver deposit, north-central Nevada. Econ. Geol. Bull. Soc. Econ. Geol. 98 (2), 425–463.
Johnson, J.W., Oelkers, E.H., Helgeson, H.C., 1992. SUPCRT92: A software package for calculating the standard molal thermodynamic properties of minerals, gases, aqueous species, and reactions from 1 to 5000 bar and 0 to 1000°C. Comput. Geosci. 18 (7), 899–947.
Kestin, J., Sengers, J.V., Kamgar-Parsi, B., Sengers, J.M.H.L., 1984. Thermophysical properties of fluid $H_2O$. J. Physi. Chem. Ref. Data 13 (1), 175–183.
Krohn, M.D., Kendall, C., Evans, J.R., Fries, T.L., 1993. Relations of ammonium minerals at several hydrothermal systems in the western united-states. J. Volcanol. Geotherm. Res. 56, 401–413.
Liu, W., Etschmann, B., Testemale, D., Hazemann, J.-L., Rempel, K., Müller, H., Brugger, J., 2014. Gold transport in hydrothermal fluids: competition among the Cl−, Br−, HS− and NH3(aq) ligands. Chem. Geol. 376, 11–19.
Loucks, R.R., Mavrogenes, J.A., 1999. Gold solubility in supercritical hydrothermal brines measured in synthetic fluid inclusions. Science 284, 2159–2163.
Marshall, W.L., Franck, E.U., 1981. Ion product of water substance, 0–1000 °C, 1–10,000 bars New International Formulation and its background. J. Physi. Chem. Ref. Data 10 (2), 295–304.
Mei, Y., Liu, W., Brugger, J., Guan, Q., 2020. Gold solubility in alkaline and ammonia-rich hydrothermal fluids: insights from ab initio molecular dynamics simulations. Geochim. Cosmochim. Acta 291, 62–78.
Migdisov, A.A., Williams-Jones, A.E., 2007. An experimental study of the solubility and speciation of neodymium (III) fluoride in F-bearing aqueous solutions. Geochim. Cosmochim. Acta 71 (12), 3056–3069.
Nilsson, K.B., Persson, I., Kessler, V.G., 2006. Coordination chemistry of the solvated AgI and AuI ions in liquid and aqueous ammonia, trialkyl and triphenyl phosphite, and Tri-n-butylphosphine solutions. Inorg. Chem. 45 (17), 6912–6921.
Oelkers, E.H., Helgeson, H.C., 1990. Triple-ion anions and polynuclear complexing in supercritical electrolyte solutions. Geochim. Cosmochim. Acta 54 (3), 727–738.
Oelkers, E.H., Helgeson, H.C., 1991. Calculation of activity coefficients and degrees of formation of neutral ion pairs in supercritical electrolyte solutions. Geochim. Cosmochim. Acta 55 (5), 1235–1251.
Pirajno, F., 2020. Subaerial hot springs and near-surface hydrothermal mineral systems past and present, and possible extraterrestrial analogues. Geosci. Front. 11, 1549–1569.
Ridgway, J., Appleton, J.D., Levinson, A.A., 1990. Ammonium geochemistry in mineral exploration—a comparison of results from the American cordilleras and the southwest Pacific. Appl. Geochem. 5, 475–489.
Ridgway, J., Martiny, B., Gomez-Caballero, A., Macias-Romo, C., Villasenor-Cabral, M. G., 1991. Ammonium geochemistry of some Mexican silver deposits. J. Geochem. Explor. 40, 311–327.
Robie, R.A., Hemingway, B.S., 1995. Thermodynamic properties of minerals and related substances at 298.15 K and 1 bar ($10^5$ pascals) pressure and at higher temperatures.
Shenberger, D.M., Barnes, H.L., 1989. Solubility of gold in aqueous sulfide solutions from 150 to 350°C. Geochim. Cosmochim. Acta 53, 269–278.
Shock, E.L., Sassani, D.C., Willis, M., Sverjensky, D.A., 1997. Inorganic species in geologic fluids: correlations among standard molal thermodynamic properties of aqueous ions and hydroxide complexes. Geochim. Cosmochim. Acta 61 (5), 907–950.
Shvarov, Y.V., 2008. HCh: New potentialities for the thermodynamic simulation of geochemical systems offered by windows. Geochem. Int. 46 (8), 834–839.
Shvarov, Y., 2015. A suite of programs, OptimA, OptimB, OptimC, and OptimS compatible with the Unitherm database, for deriving the thermodynamic properties of aqueous species from solubility, potentiometry and spectroscopy measurements. Appl. Geochem. 55, 17–27.
Simmons, S.F., White, N.C., John, D.A. (2005) Geological Characteristics of Epithermal Precious and Base Metal Deposits, Economic Geology, Society of Economic Geologists, 100th Anniversary Volume, 485-522.
Simpson, M.P., Christie, A.B., 2019. Hydrothermal alteration mineralogical footprints for New Zealand epithermal Au-Ag deposits. N. Z. J. Geol. Geophys. 62 (4), 483–512.
Skibsted, L., Bjerrum, J., 1974. Studies on gold complexes. I. Robustness, stability and acid dissociation of the tetrammine gold (III) ion. Acta Chem. Scand 28 (1–2), 740–746.
Soechting, W., Rubinstein, N., Godeas, M., 2008. Identification of ammonium-bearing minerals by shortwave infrared reflectance spectroscopy at the Esquel gold deposit, Argentina. Econ. Geol. 103 (4), 865–869.
Stefánsson, A., Seward, T.M., 2004. Gold(I) complexing in aqueous sulphide solutions to 500°C at 500 bar. Geochim. Cosmochim. Acta 68, 4121–4143.
Sverjensky, D.A., Shock, E.L., Helgeson, H.C., 1997. Prediction of the thermodynamic properties of aqueous metal complexes to 1000°C and 5 kb. Geochim. Cosmochim. Acta 61 (7), 1359–1412.
Tagirov, B.R., Zotov, A.V., Akinfiev, N.N., 1997. Experimental study of dissociation of HCl from 350 to 500°C and from 500 to 2500 bars: Thermodynamic properties of HCl°(aq). Geochim. Cosmochim. Acta 61 (20), 4267–4280.
Valentino, G.M., Cortecci, G., Franco, E., Stanzione, D., 1999. Chemical and isotopic compositions of minerals and waters from the Campi Flegrei volcanic system, Naples, Italy. *J. Volcanol. Geotherm. Res.* 91, 329–344.
Wang, X.-S., Timofeev, A., Williams-Jones, A.E., Shang, L.-B., Bi, X.-W., 2019. An experimental study of the solubility and speciation of tungsten in NaCl-bearing aqueous solutions at 250, 300, and 350 °C. Geochim. Cosmochim. Acta 265, 313–329.
White, N.C., Hedenquist, J.W., 1995. Epithermal gold deposits: styles, characteristics and exploration. SEG Discovery 1–13.
Williams-Jones, A.E., Bowell, R.J., Migdisov, A.A., 2009. Gold in solution. Elements 5, 281–287.
Williams-Jones, A., Migdisov, A., 2014. Experimental constraints on the transport and deposition of metals in ore-forming hydrothermal systems. Soc. Econ. Geol. 18, 77–96.
Wood, S.A., Mountain, B.W., Pan, P., 1992. The aqueous geochemistry of platinum, palladium and gold; recent experimental constraints and a re-evaluation of theoretical predictions. Can. Mineral. 30 (4), 955–982.